Journal of Nuclear Science and Technology

ISSN: (Print) (Online) Journal homepage: https://www.tandfonline.com/loi/tnst20

Measurements of capture cross-section of ^{93}Nb by activation method and half-life of ^{94}Nb by mass analysis

Shoji Nakamura, Yuji Shibahara, Shunsuke Endo & Atsushi Kimura

To cite this article: Shoji Nakamura, Yuji Shibahara, Shunsuke Endo & Atsushi Kimura (2023) Measurements of capture cross-section of ^{93}Nb by activation method and half-life of ^{94}Nb by mass analysis, Journal of Nuclear Science and Technology, 60:11, 1361-1371, DOI: 10.1080/00223131.2023.2198526

To link to this article: https://doi.org/10.1080/00223131.2023.2198526

JOURNAL OF NUCLEAR SCIENCE AND TECHNOLOGY
2023, VOL. 60, NO. 11, 1361–1371
https://doi.org/10.1080/00223131.2023.2198526

Taylor & Francis
Taylor & Francis Group

ARTICLE

Measurements of capture cross-section of ^{93}Nb by activation method and half-life of ^{94}Nb by mass analysis

Shoji Nakamura[a], Yuji Shibahara[b], Shunsuke Endo[a] and Atsushi Kimura[a]

[a]Nuclear Data Center, Nuclear Science and Engineering Center, Japan Atomic Energy Agency, Tokai-mura, Naka-gun, Ibaraki-ken, Japan; [b]Radioactive, Waste Management, Division of Nuclear Engineering Science, Institute for Integrated Radiation and Nuclear Science, Kyoto University, Kumatori-cho, Sennan-gun, Osaka, Japan

ABSTRACT

The thermal-neutron capture cross section (σ_0) and resonance integral (I_0) for ^{93}Nb were measured by an activation method; a half-life of ^{94}Nb was derived by mass analysis. Niobium-93 samples were irradiated with the use of the hydraulic conveyer installed in the research reactor in Institute for Integral Radiation and Nuclear Science, Kyoto University. Gold-aluminum and cobalt-aluminum alloy wires were used to monitor thermal-neutron fluxes and *Westcott*'s indexes at the irradiation position. A 25-μm-thick gadolinium foil was used to separate reactions ascribed to thermal neutrons. Its thickness provided a cut-off energy of 0.133 eV. In order to attenuate the radioactivity of ^{182}Ta produced by impurities, the Nb samples were cooled for nearly 2 years. The induced radio activity in the monitors and Nb samples was measured by gamma-ray spectroscopy. In the analysis based on *Westcott*'s convention, the σ_0 and I_0 values were calculated as 1.11 ± 0.04 barns and 10.5 ± 0.6 barns, respectively. After the γ-ray measurements, mass analysis was applied to the Nb samples to obtain the reaction rate. By combining data obtained by both γ-ray spectroscopy and mass analysis, a half-life of ^{94}Nb was determined as $(2.00 \pm 0.15) \times 10^4$ years.

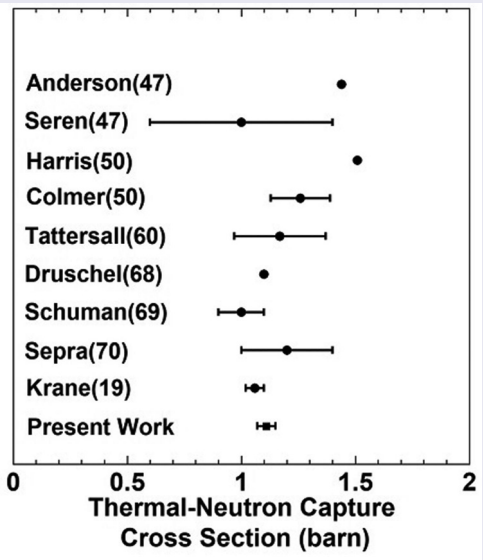

ARTICLE HISTORY
Received 16 December 2022
Accepted 24 March 2023

KEYWORDS
Niobium-93; niobium-94; thermal-neuron capture cross section; resonance integral; activation method; mass analysis; Kyoto University research reactor

1. Introduction

Since the first commercial nuclear power plant went into operation in 1966 in Japan, light water reactors have been actively constructed. The unavoidable issue that arises after more than half a century is decommissioning nuclear reactors, which have reached the end of their service lives. Decommissioning will be an issue, especially in terms of environmental impact, when disposing of radioactive industrial waste: concrete, fuel control materials, structural materials and electric cables, coming from nuclear reactor facilities. Important radionuclides in decommissioning have been identified, and the concept of clearance levels [1] has been discussed for those nuclides. Regarding structural materials, niobium-94 is listed as one of the radionuclides with defined clearance levels, because a small amount of Nb (0.8–0.9%) is intentionally added in structural materials for improving material performance. The clearance level of ^{94}Nb is a radioactivity concentration of 0.1 Bq/g. Reactor

CONTACT Shoji Nakamura nakamura.shoji@jaea.go.jp Nuclear Data Center, Nuclear Science and Engineering Center, Japan Atomic Energy Agency, 2-4 Shirakata, Tokai-mura, Naka-gun, Ibaraki-ken, Japan

structural stainless steel (18–8 stainless steel: A.I.S.I. Type 304, 304 L) and niobium-containing stainless steel (A.I.S.I. Type 347) have been used in various structures such as pressure vessels, pipes, and fuel cladding due to their excellent heat and corrosion resistance. Austenitic stainless steel (SUS316) has been selected as a material for fuel cladding and wrapper tubes for fast reactors, and strength at high temperature was improved by adding a small amount (0.1%) of ^{93}Nb in the stainless steels. Although niobium-93 has a small thermal-neutron capture cross section (1.15 ± 0.05 barns [2], 1.142 barns [3]), it can be activated by reactor neutrons and generates ^{94}Nb with a relatively long half-life ($T_{1/2}$) of 20,400 years [4]. A partial decay scheme of ^{94}Nb [5] is shown in Figure 1. The activated Nb therefore continues to emit gamma rays over a very long period of time. Corrosion products containing Nb can contaminate heat transfer mediums, creating an obstacle to reactor maintenance due to the radiation dose and to disposal in decommissioning. Therefore, it becomes necessary to evaluate the amount of ^{94}Nb produced by neutron irradiation.

Here, we summarize the present situation of thermal-neutron capture cross-section data of ^{93}Nb. The reported data so far are plotted in Figure 2. The measurement data [6–13] are old, with few measurements in the last 50 years; in recent years, one measurement has been reported in 2019 [14]. The principal values of the reported data are not convergent, and their uncertainties are as large as 15–20%. The magnitude of the uncertainty will affect the uncertainty of the predicted amount of ^{94}Nb radioactivity. Consequently, the present study measured the thermal-neutron capture cross section (σ_0) of ^{93}Nb that contributes to the evaluation of the produced amount of ^{94}Nb. The cross section was derived with an accuracy of several percent, higher than the previously reported values. This causes the reported σ_0 data to converge. Furthermore, a resonance integral (I_0) was derived in the process of deriving σ_0. As in the past

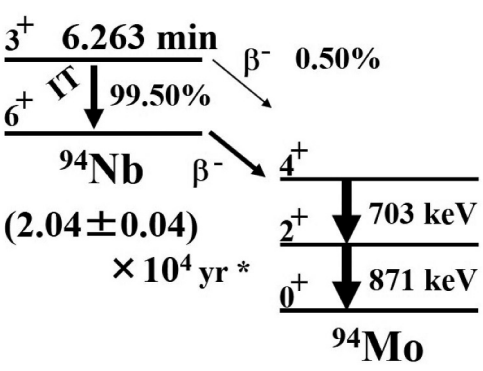

Figure 1. Partial decay scheme for ^{94}Nb [5]. * The half-life of the ^{94}Nb ground state was taken from Ref. [4].

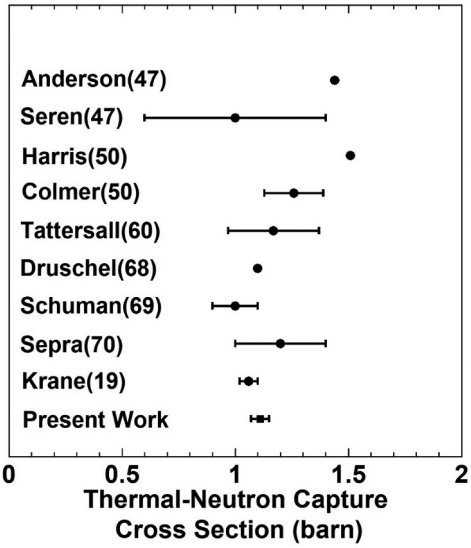

Figure 2. Thermal-neutron capture cross sections for ^{93}Nb plotted in order of publication year [6–14]. Past reported data are denoted by closed circles (●), and the present work by closed square (■).

measurements an activation method and gamma-ray spectroscopy were used with reactor neutrons, but in this work mass analysis was also conducted to cross-check the reaction rate of ^{93}Nb. In the process of mass analysis, a measurement of the half-life of ^{94}Nb was also determined.

2. Experimental principle

Our experimental method based on *Westcott's* convention is described here for deriving the thermal-neutron capture cross section and resonance integral. A simple outline of the convention is presented, and further details are described elsewhere [15,16]. When a neutron flux in a nuclear reactor is well moderated, it is assumed that the neutron flux distribution can be represented by the sum of two components: a Maxwell distribution and an epi-thermal component. The reaction rate R can be expressed in the simple form [17]:

$$R/\sigma_0 = gG_{th}\phi_1 + G_{epi}\phi_2 s_0 \qquad (1)$$

where σ_0 is the thermal-neutron capture cross section; the factor g is a function of temperature, related to the departure of the cross-section behavior from the 1/υ law; ϕ_1 is the neutron flux component in the thermal energy region; the symbol ϕ_2 is that in the epi-thermal energy region. The symbols G_{th} and G_{epi} denote self-shielding coefficients for thermal- and epi-thermal neutrons, respectively. These self-shielding coefficients [18,19] are calculated from the neutron capture cross sections and areal densities of the samples. The parameter s_0 represents the sensitivity to epi-thermal neutrons and is defined by:

$$s_0 = \frac{2I_0'}{\sqrt{\pi}\sigma_0} \quad (2)$$

where I_0' is called a "reduced resonance integral," which is the quantity obtained by subtracting a 1/υ-contribution from a resonance integral I_0. The resonance integral I_0 is a quantity indicating the likelihood of a capture reaction by epi-thermal neutrons. The resonance integral I_0 is then given by adding the 1/υ-contribution to the reduced resonance integral I'_0:

$$I_0 = I_0' + I(1/v) \quad (3)$$

where the term $I_{(1/\upsilon)}$ is the 1/υ-contribution to I_0 above a (cadmium) cut-off energy E_c. The term $I_{(1/\upsilon)}$ is given by:

$$I_{(1/v)} = 2g\sigma_0\sqrt{\frac{E_0}{E_C}} \quad (4)$$

where E_0 is the thermal-neutron energy of 0.0253 eV. Here, in order to find the two quantities for σ_0 and s_0 (or I_0) of a target nuclide, one more equation should be required in addition to Eq. (1). When using the neutron field in a nuclear reactor, reaction rates are obtained by artificially changing the neutron field with a neutron filter such as cadmium (Cd) or gadolinium (Gd). The reaction rate in this case can be written in the same manner as Eq. (1):

$$R'/\sigma_0 = G_{th}\phi_1' + G_{epi}\phi_2' s_0 \quad (5)$$

for the filtered target. Here, the prime (') means irradiation with Cd or Gd filters. The symbols ϕ_1' and ϕ_2' are neutron flux components in thermal- and epi-thermal energy regions. The neutron flux components in Eqs. (1) and (5) are obtained using nuclides such as ^{59}Co and ^{197}Au, whose thermal-neutron capture cross sections and decay data are well known. Solving Eqs. (1) and (5) provides the σ_0 and parameter s_0. The resonance integral I_0 can be obtained by using the obtained value for s_0 and Eqs. (2-4). In this study, the reaction rate R' in Eq. (5) was measured by shielding the thermal neutron component using a Gd filter. A 25-μm-thickness Gd foil was chosen to take a value of 0.133 eV as the cut-off energy E_c [20]. For this cut-off energy E_c, the 1/υ contribution to the I_0 is found by Eq. (4) to be 0.872 $g\sigma_0$.

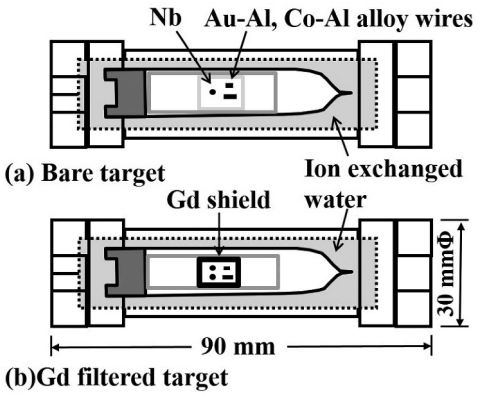

Figure 3. Schematic of irradiation capsules containing bare and Gd filtered targets.

3. Experiments

3.1. Target preparation

Figure 3 shows an overview of prepared ^{93}Nb targets. The niobium samples were metal foils with a purity of 99.99%; each had a diameter of 4 mm, a thickness of 0.054 mm, and a mass in the order of 5 mg. The weights of the Nb samples were measured with an accuracy of ±1 μg with a microbalance: model XP6 (METTLER TOLEDO, United States). A set of a gold-aluminum (Au-Al) alloy wire (content ratio 0.112 ± 0.001%, purity of contained Au 99.98%, 0.510 mm in diameter) and a cobalt-aluminum (Co-Al) alloy wire (content ratio 0.460 ± 0.005%, purity of contained Co 99.93%, 0.381 mm in diameter) was used to monitor neutron flux components at the irradiation position. These two wire choices are suitable for flux monitors because ^{59}Co and ^{197}Au have different sensitivities to thermal- and epi-thermal neutrons. The amount of ^{59}Co and ^{197}Au contained in each wire was determined by their content ratios and weight measurements with the microbalance. Information on Nb foils and alloy wires is summarized in Table 1. These neutron flux monitor wires were the same as in Ref [17] because they were shared for neutron irradiation. The set of ^{59}Co and ^{197}Au monitors was attached near to the ^{93}Nb sample and then wrapped with a 15-μm-thick high-purity Al foil. The ^{93}Nb sample with the monitor set was used as an irradiation target (called 'a bare target' as shown in Figure 3(a)). Another monitor set was attached near two other

Table 1. Niobium samples and neutron flux monitors for the irradiations.

Nuclide	Shape and Size	Abundance (%)	Purity (%)	Weight (mg)	Irradiation Time (sec)
^{93}Nb	Metal foil 4 mmϕ, 0.054 mm^{t}	100	99.9	5.090 ± 0.001[a)] 10.126 ± 0.002[b)] †	19,595[a)] 19,585[b)]
^{59}Co	Co-Al alloy wire 0.381 mmϕ, 1 mm	0.460 ± 0.005	99.93	0.275 ± 0.001[a)] 0.444 ± 0.001[b)]	
^{197}Au	Au-Al alloy wire 0.510 mmϕ, 1 mm	0.112 ± 0.001	99.98	0.473 ± 0.001[a)] 0.390 ± 0.001[b)]	

a) In the case of 'a bare target.' b) In the case of 'a Gd filtered target.'
† Two Nb foils were used to obtain sufficient statistics.

^{93}Nb samples, and they were wrapped with Al foil. The wrapped samples were sandwiched with a 25-μm-thick Gd foil with a purity 99.9% (called 'a Gd filtered target' as shown in Figure 3(b)) to subtract the contribution from thermal neutrons as described in Section 2. The bare and Gd filtered targets were placed into aluminum inner capsules filled with helium gas. The inner capsules containing the targets were then placed into outer capsules made of aluminum alloy (A5052) used for the hydraulic conveyer. Just before irradiations the outer capsules were filled with ion exchanged water and the lids were then closed firmly.

3.2. Neutron irradiation in hydraulic conveyer

The neutron irradiation was carried out with neutrons supplied by the research reactor (KUR) of the Institute for Integrated Radiation and Nuclear Science, Kyoto University (KURNS) [21]. In examining the ^{93}Nb(n, γ)^{94}Nb reaction, it is necessary to produce as much ^{94}Nb as possible to obtain a sufficient yield of gamma rays, since ^{94}Nb has a thermal-neutron capture cross-section on the order of 1 barn and also a relatively long half-life of 20,400 years. Thus, neutron irradiation was performed with a hydraulic conveyer system as shown Figure 4 in order to access a large neutron flux of 1×10^{14} n/cm^{2}sec in 5-MW power operation of the KUR; however, the irradiation was limited to 6 h on a single day once per week. The present irradiations were performed under the same conditions as those in Ref [17]. The bare target was transported from the top of the KUR to the center of the reactor core by sending out the wire of the conveyer system. The bare target was irradiated for 6 h in 5-MW power operation. After irradiation, the capsule was transferred to a canal in the hot cave room of the KUR, and then cooled for 3 days, mainly to attenuate the induced radioactivity of the capsule itself. The Gd filtered target was also irradiated and cooled in the same procedure during the 5-MW operating day of the next week.

3.3. Gamma-ray measurement

After cooling, the irradiated targets were opened in a cell at the hot laboratory of the KUR, and the ^{93}Nb samples and the neutron flux monitors were collected from the capsules. Gamma-ray measurements were performed on ^{93}Nb samples and neutron flux monitors. Decay gamma rays emitted from ^{93}Nb samples and monitors were measured with the high-purity Ge detector (model GEM 25,185; ORTEC, United States) installed in the first measurement room of the hot laboratory. The measurement distance was 100 mm from the front surface of the Ge detector to the sample position. Gamma-ray peak efficiencies of the Ge detector were measured with a mixed source AM-8140 supplied by Eckert & Ziegler Nuclitec GmbH, Germany. The uncertainty of the source activity was 1.5% (1σ). Figure 5 shows the gamma-ray spectrum of the bare Nb sample measured about 5 days after irradiation. Decay gamma rays originating from ^{94}Nb were observed at 703 keV and 871 keV with poor statistics relative to intense background gamma rays originating from ^{182}Ta ($T_{1/2}$ = 114.43 days [22]). Many gamma rays emitted from ^{182}Ta were observed in the energy regions below 500 keV and above 1 MeV. This is because even a high-purity Nb sample contains a very small amount of ^{181}Ta, which has a relatively large neutron capture cross section of 20.4 ± 0.3 barn [2] and thus the Nb sample produces a large amount of ^{182}Ta. In order to improve the statistics and obtain accurate gamma-ray yields for ^{94}Nb, it was decided to cool the Nb samples for about 2 years thereby attenuating ^{182}Ta activity sufficiently. After cooling the irradiated Nb samples, the emitted decay gamma rays

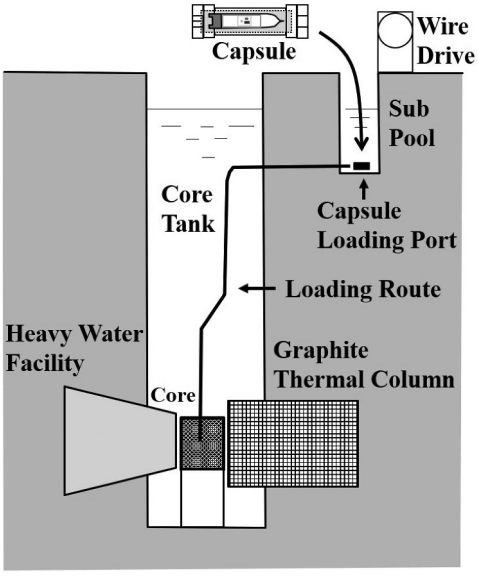

Figure 4. Outline of the hydraulic conveyer system in the KUR.

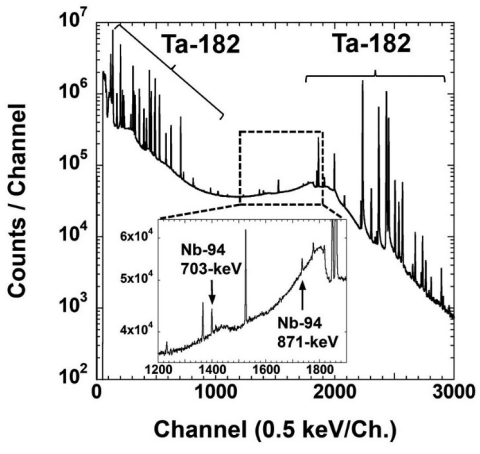

Figure 5. Gamma-ray spectrum of the bare Nb sample. Cooling time was about 5 days; live time was 65,535 sec and real time was 70,372 sec; dead time was 7%.

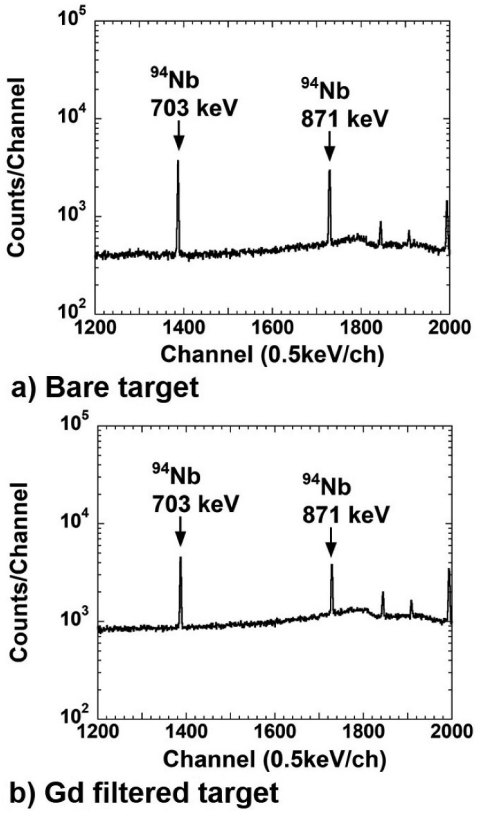

Figure 6. Spectra of γ rays emitted from the (a) bare and (b) Gd filtered ^{93}Nb samples. Caption: (a) Cooling time was 696 days; live time was 36,000 sec and real time was 36,043 sec. (b) Cooling time was 675 days; live time was 54,000 sec and real time was 54,093 sec.

were remeasured for 10 h for the bare target and 15 h for the Gd filtered target. The spectra obtained for these targets are drawn in Figure 6.

4. Analysis and results

4.1 Neutron flux components

The neutron flux components were derived for the irradiation position of the hydraulic conveyer as follows: The reaction rates R and R' were obtained from gamma-ray yields emitted from the irradiated flux monitors. Table 2 summarizes the nuclear data used in this analysis. Using the obtained reaction rates of the monitors, neutron flux components were determined using Eqs. (1) and (5) in *Section 2*. Figure 7 plots the neutron fluxes obtained by the monitor wires against the parameter s_0. The neutron flux components ϕ_1 and ϕ_1' are derived from the relations shown in Figure 7; the slopes of the solid lines give the epi-thermal flux components: ϕ_2 and ϕ_2'. The intercept on the y-axis in Figure 7 gives the thermal-neutron flux component ϕ_1, which was found to be $(1.09 \pm 0.02) \times 10^{14}$ $n/cm^2/sec$ in the present experiment. The proportion of epi-thermal neutrons was found to be 3.3%. Table 3 summarizes the results of the neutron flux components ϕ_1, ϕ_2, ϕ_1' and ϕ_2' together with the reaction rates R and R' of the flux monitors, and Table 4 summarizes the statistical and systematic uncertainties for the flux monitor measurements.

4.2. ^{93}Nb cross section by gamma-ray analysis

This section describes the study of the neutron capture reaction of ^{93}Nb by gamma-ray analysis. From the decay scheme in Figure 1, it can be seen that the isomeric state ^{94m}Nb with a half-life of 6.263-min transitions to the ground state ^{94g}Nb with a probability of 95.50%, and the remaining 0.50% decays to ^{94}Mo. At the time of gamma-ray analysis, the isomer ^{94m}Nb had fully decayed to ^{94g}Nb because the irradiated Nb samples were sufficiently cooled. Thus, it was considered that the yields of gamma rays emitted from ^{94g}Nb reflected the production amount of both the isomeric and ground states; however, regarding the effect of the β-decay branch from the isomeric state, with a probability of at most 0.5%, this was incorporated into the systematic uncertainty. When solving the differential equation for the ^{93}Nb(n,γ)$^{94m+g}$Nb reaction, the reaction rate R and R' is given by the following equation:

$$R^{(\prime)} = \frac{\lambda_1 Y_1 \cdot (1/G_\gamma) \cdot (T_R/T_L)}{\varepsilon_{\gamma 1} I_{\gamma 1} n_0 (1 - \exp(-\lambda_1 T_{irr})) \cdot \exp(-\lambda_1 T_c) \cdot (1 - \exp(-\lambda_1 T_R))} \quad (6)$$

where subscripts 0 and 1 denote ^{93}Nb and $^{94m+g}$Nb, respectively. The symbol n is the number of nuclei in the target; for example, n_0 represents the number of ^{93}Nb nuclei, which was quantified by measuring the sample weight using the microbalance. The symbol I_γ is the gamma-ray emission probability; ε_γ is the corresponding gamma-ray detection efficiency; λ is the decay constant given by the half-life $T_{1/2}$; G_γ is the

Table 2. Nuclear data of monitors used in the present analysis [2, 4, 22].

Nuclide	Half-life[a]	Detected γ-ray: γ-ray Energy (keV)	Detected γ-ray: *Emission Probability* Iγ[a] (%)	σ_0[a] (barn)	I_0[a] (barn)	factor g	Parameter s_0[a]	G_{th}	G_{epi}
^{59}Co	5.2711 *8*	1173.2	99.9826 *6*	37.18 *6*	75.8 *20*	1.0004	1.74 *6* [b]	1.00	1.00
(to ^{60}Co)	(years)	1332.5	99.85 *3*				1.32 *6* [c]		
^{197}Au	2.6943 *3*	411.8	95.62 *6*	98.65 *9*	1550 *28*	1.0054	17.2 *3* [b]	1.00	0.99
(to ^{198}Au)	(days)						16.7 *3* [c]		
^{93}Nb	2.04 *4*	871.1	99.9 *1*	1.15 *5*	8.5 *5*	1.003		1.00	1.00
(to ^{94g}Nb)	(×10^{14} years)	702.6	97.9 *20*						

[a]In our notation, 2.6943 *3* is 2.6943 ± 0.0003, 95.62 *6* is 95.65 ± 0.06, 98.65 *9* is 98.65 ± 0.09, and *etc.*
[b]Parameter s_0 at a cut-off energy of 0.5 eV. [c] Parameter s_0 at a cut-off energy of 0.133 eV.

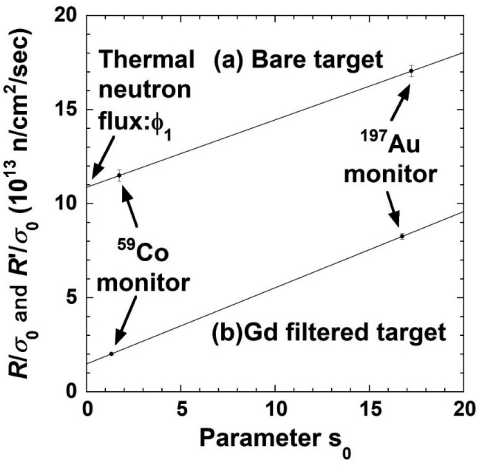

Figure 7. Relations between R/σ_0 (and R'/σ_0) and parameter s_0 obtained from irradiation at hydraulic conveyer in 5-MW power operation.

gamma-ray self-shielding coefficient; Y is the yield of gamma rays obtained by measurement. Regarding the time parameters, T_{irr} represents the irradiation time at the reactor, T_c the cooling time (or interval time) from the end of the irradiation to the start of measurement, T_R is the real time of gamma-ray measurement and T_L the live time. The reaction rates R and R' were derived using Eq. (6) from the yields of gamma rays emitted from the decay of ^{94g}Nb obtained by gamma-ray measurement of each target. Table 5 lists measurement conditions, obtained gamma-ray yields, and the reaction rates for the ^{93}Nb(n,γ)$^{94m+g}$Nb reaction. Nuclear data used for the present analysis are also summarized in Table 2. Uncertainty contributions to the reaction rates are listed in Table 6. We quantitatively examined how the influence of each of these items propagate to the reaction rates. The reaction rates and neutron flux component calculations yield values of 1.11 ± 0.04 barns for the thermal-neutron capture cross section σ_0, 9.74 ± 0.52 for the parameter s_0, and 10.5 ± 0.6 barns for the resonance integral I_0 at $Ec = 0.133$ eV. A decomposition of uncertainties propagated to the present results of σ_0 and s_0 is summarized in Table 7. The total uncertainty was evaluated by taking the square root of the sum of squares of partial uncertainties. The present results are summarized in Table 8 together with the past measured [6–14,23–26] and evaluated data [2,3].

4.3. ^{93}Nb reaction rate by mass analysis

Only 0.5% of ^{94m}Nb decay to ^{94}Mo and the remaining 99.50% of ^{94m}Nb decays to ^{94g}Nb. In other words, ^{94g}Nb bears the bulk of the information on how much capture reaction has occurred. Furthermore, it would be possible to derive the reaction rate of ^{94}Nb by determining the isotope ratio of ^{94}Nb to ^{94}Nb. We therefore set out to

Table 3. Reaction rates of flux monitors and neutron flux components at the irradiation position in the core of KUR [17].

Target Type	R/σ_0 and R'/σ_0 ($\times10^{13}$/cm^2/sec)		flux components ($\times10^{14}$ n/cm^2/sec)	
	^{59}Co	^{197}Au	ϕ_1 and ϕ_1'	ϕ_2 and ϕ_2'
Bare	11.5 ± 0.2	17.1 ± 0.3	1.09 ± 0.03	0.036 ± 0.003
Gd filtered	2.02 ± 0.04	8.27 ± 0.15	0.149 ± 0.005	0.041 ± 0.001

Table 4. Systematic uncertainties for flux monitor measurements.

Items	Uncertainties (%)	
	^{59}Co	^{197}Au
Cross section: σ_0	0.16	0.09
Half-life: $T_{1/2}$	0.01	0.01
Emission probability: I_γ	0.03	0.06
Weight: m	0.36	0.20
Abundance (*wt*%)	1.09	0.89
Efficiency: ε_γ,fitting uc. only*	0.16	0.28
fitting + source uc. (1.5%)	1.51	1.53
Total systematic uncertainty	1.91	1.78

*These systematic uncertainties due to the calibration source uncertainty are canceled at the time of division of reaction rates.

Table 5. Experimental conditions, obtained gamma-ray yields and reaction rates for the ^{93}Nb(n,γ)$^{94m+g}$Nb reaction.

Target	Irrad. time T_{irr} (sec)	Cooling time T_c (day)	Measur. time T_L, T_R (sec)	Peak Efficiencies (%)	-ray yield Y (Counts)	Reaction rate * R or R' ($\times10^{-10}$/sec)	Arithmetic mean R or R' ($\times10^{-10}$/sec)
Bare	19,595	695.65	36,000	0.2577 (703 keV)	10121 ± 130	1.601 ± 0.021	1.598±0.016 (±0.046 †)
			36,043	0.2161 (871keV)	8665± 135	1.594 ± 0.025	
Gd filtered	19,585	675.07	54,000		11370±164	0.6031±0.0870	0.6027±0.071 (±0.0176 †)
			54,093		9719± 183	0.6023±0.1134	

* Statistical uncertainties are only listed. † Systematic uncertainties: see Table 6 for the details.

Table 6. Uncertainties propagated to the reaction rates due to uncertainties of the data used in the present analysis for the ^{94}Nb (n,γ)$^{94m+g}$Nb reaction.

Concerned Items	Uncertainties (%)
Half-life of ^{94g}Nb: $T_{1/2} = 2.04 \pm 0.04 \times 10^{14}$years	1.96
Emission probability: I_γ(871 keV) 99.9%	0.1
Isomer transition: 99.50%	0.5
Efficiency: ε_γ(871 keV) fitting uc.+ source uc. (1.5%)	1.68
(fitting uc. only)	(0.75)
Sample weight: m (mg)	0.02
Irradiation time: T_{irr}	0.46
Total systematic uncertainty	2.67
Uncertainty when considering R/R' ratio	0.88

Table 7. Partial uncertainties propagated to the σ_0 and parameter s_0.

σ_0 (barn)	Partial Uncertainties*		Parameter s_0	Partial Uncertainties*	
1.11 ± 0.04	∂ (σ_0 /R)	0.0317	9.74 ± 0.52	∂ (s_0 /(R/R'))	0.1100
	∂ (σ_0 /ϕ_1)	0.0122		∂ (s_0 /ϕ_1)	0.2218
	∂ (σ_0 /ϕ_2)	0.0122		∂ (s_0 /ϕ_2)	0.2225
	∂ (σ_0 /s_0)	0.0144		∂ (s_0 /ϕ_1')	0.1490
				∂ (s_0 /ϕ_2')	0.3702

*In our notation, ∂ (σ_0/R) denotes partial differentiation of σ_0 by R.

Table 8. Present results of the thermal-neutron capture cross section and the resonance integral for the ^{93}Nb(n,γ)$^{94m+g}$Nb reaction together with the past reported data.

Author	σ_0 (barn)	I_0 (barn)	Cut-off energy (eV)	Ref.
Present Work	**1.11 ± 0.04**	**10.1 ± 0.6***	**0.5**	
		10.5 ± 0.6	**0.133**	
		(s_0 = 9.74 ± 0.52)		
Krane (2019)	1.06 ± 0.04	10.8 ± 1.1	0.5	[14]
Mughabghab (2018)†	1.15 ± 0.05	8.83 ± 0.40	0.5	[2]
JENDL-4.0 (2011)†	1.142	8.982	0.5	[3]
Serpa (1970)	1.2 ± 0.2			[13]
Shuman (1969)	1.0 ± 0.1	8.5 ± 0.5	0.5	[12]
Hayodom (1969)		5.8	0.5	[23]
Druschel (1968)	1.1	8.5	0.5	[11]
Lesage (1966)		18.8 ± 3.0		[24]
Feiner (1961)		13.8 ± 2.2	0.55	[25]
Tattersall (1960)	1.17 ± 0.02	13 ± 5	0.67	[10]
Macklin (1955)		3.87, 8.3		[26]
Colmer (1950)	1.26 ± 0.13			[9]
Harris (1950)	1.51	4.19	0.5	[8]
Seren (1947)	1.0 ± 0.4			[7]
Anderson (1947)	1.44			[6]

* Result of re-calculation at 0.5 eV as defined. † *Evaluation*.

determine the reaction rate by mass analysis. Using the same description as given in *Section 4.2*, the number of nuclei of produced ^{94}Nb is given by the following simple equation:

$$n_1 = n_0 \cdot R \cdot T_{irr} \tag{7}$$

This gives the reaction rate R as follows:

$$R = \frac{n_1}{n_0 \cdot T_{irr}} = \frac{r_{mass}}{T_{irr}} \tag{8}$$

where r_{mass} is the isotope ratio of ^{94}Nb to ^{93}Nb. Equation (8) indicates that the reaction rate can be obtained with a precision determined by that of the mass analysis. It is trivial to see that Eq. (8) is not affected by uncertainties of nuclear data used for other analyses, such as half-life data and gamma-ray emission probabilities.

The bare and Gd filtered Nb samples were dissolved in 0.2 M HF +3 M HNO_3 and then each solution was analyzed by thermal ionization mass spectrometry (TIMS) [27]. The analysis was performed using the mass spectrometer TRITON-T1 [28–32] (Thermo Fisher Scientific, Inc. U.S.A.) installed at KURNS. The isotope analysis of Nb was performed by the double filament method with a 'zone-refined' rhenium filament [27]. Here, attention was focused on the ionization potential of Nb. The ionization potentials of Mo and Zr were also examined, since Mo and Zr belong to the transition elements, like Nb, and they are elements adjacent to Nb. The ionization potential energy of Nb is 6.8 eV, while the energies of Mo and Zr, respectively, are 7.1 eV and 6.6 eV [33], which are close to that of Nb. We used silica gel + H_3BO_3 [27] as additives for the analysis of Mo and Zr in this mass analysis. The rhenium filaments were drip coated with

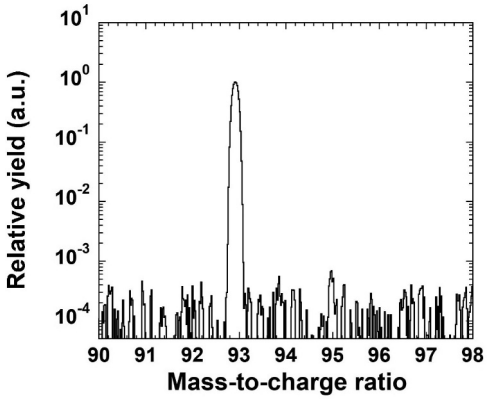

Figure 8. An example of mass spectra obtained using an unirradiated Nb sample.

Nb solution, dried, and then set into the spectrometer. Figure 8 shows an example of mass spectra obtained using an unirradiated Nb sample in order to adjust the analytical conditions. The abscissa is the mass-to-charge ratio (m/z) which is the value obtained by dividing the ion mass (m) by the number of charges (z), and the ordinate is the yield. In the mass analysis of irradiated Nb samples, ions of ^{93}Nb were detected with a Faraday cup and ^{94}Nb were detected simultaneously with a secondary electron multiplier. It should be noted that the yield at $m/z = 94$ is possibly due to isobaric interference by ^{94}Zr and ^{94}Mo. However, the yield at m/z = 93 is only ^{93}Nb. Interference from other impurities was found to be negligibly small. Thus, isobaric interferences by Zr and Mo were evaluated using their natural abundances. First, it was confirmed that the isotopic ratios of ^{90}Zr to ^{91}Zr, and of ^{98}Mo to ^{100}Mo in the mass spectrum were consistent with natural abundances of Zr and Mo. Next, the contribution of ^{94}Zr to ^{94}X (a substance X with mass number 94) was evaluated from the natural abundances of ^{94}Zr and ^{94}Zr, and the yield ratio of ^{90}Zr to ^{94}Nb obtained from the mass spectrum; similarly, the contribution of ^{94}Mo to ^{94}X was evaluated from the natural abundances of ^{94}Mo and ^{98}Mo, and the yield ratio of ^{98}Mo to ^{93}Nb was obtained from the spectrum. Then, considering the yield ratio of X and ^{93}Nb, the ^{94}Nb/^{93}Nb isotope ratio (r_{mass}) of the Nb sample is presented by:

$$r_{mass} = {}^{94}Nb/{}^{93}Nb = \left({}^{94}X - \left({}^{94}Zr + {}^{94}Mo\right)\right)/{}^{93}Nb \tag{9}$$

Finally, using the ^{94}Nb/^{93}Nb ratio before and after neutron irradiation, the production of ^{94}Nb was evaluated by the following equation:

$$\left[\left({}^{94}X - \left({}^{94}Zr + {}^{94}Mo\right)\right)/{}^{93}Nb\right]_{after} - \left[\left({}^{94}X - \left({}^{94}Zr + {}^{94}Mo\right)\right)/{}^{93}Nb\right]_{before} \tag{10}$$

Here, a difference is taken in order to prevent the amount of (^{94}Zr+^{94}Mo) from being missed and/or oversubtracted, because the term [^{94}X - (^{94}Zr+^{94}-Mo)/^{93}Nb]$_{before}$ in Eq.(10) may be nonzero due to analysis uncertainties. The isotope ratio r_{mass} for the bare target was $(3.07 \pm 0.21) \times 10^{-6}$; however, in the case of the Gd filtered target, because the amount ^{94}Nb was very small, the isotope ratio could not be obtained as accurately, yielding a result of $(5.8 \pm 2.9) \times 10^{-7}$. That is why only the reaction rate R of the bare target was obtained using Eq. (8) and found to be $(1.567 \pm 0.107) \times 10^{-10}$/sec with a T_{irr} of 19,595 s. In comparison, the reaction rate obtained by γ-ray measurement from the result in Table 5 was $(1.598 \pm 0.046) \times 10^{-10}$/sec which includes the systematic uncertainty of 2.67%. The result from mass analysis is in agreement with that from γ-ray measurement within the limit of uncertainty.

4.4. Half-life of ^{94}Nb

In the preceding *Subsections*, the reaction rate was examined using different methods: gamma-ray spectroscopy and mass analysis. The equations of the reaction rates given by the different methods are equal to each other, so they may be written as follows:

$$\frac{Y_1}{\varepsilon_\gamma \cdot I_\gamma \cdot n_0 \cdot \lambda_1 \cdot T_{irr} \cdot T_L} = \frac{r_{mass}}{T_{irr}} \tag{11}$$

where the symbols have the same meaning as before. Rewriting the decay constant λ_1 of ^{94g}Nb with the half-life $T_{1/2}$ gives the following:

$$T_{1/2} = r_{mass} \cdot \frac{\varepsilon_\gamma \cdot I_\gamma \cdot n_0 \cdot \ln(2) \cdot T_L}{Y_1} \tag{12}$$

It is possible to derive the half-life from the gamma-ray yield and isotope ratio obtained with an appropriate measurement time, without observing the decay of gamma rays over a very long period of time. Using the data from the present experiment, the half-life of ^{94g}Nb was determined from the 703-keV and 871-keV γ-rays, and the same results were obtained from these two transitions of $(2.00 \pm 0.15) \times 10^4$ years. Here, in addition to the statistical uncertainty in the gamma-ray yield (see Table 5), we considered systematic uncertainties for the isotope ratio, detection efficiency, gamma-ray emission probability, and sample mass (see Table 6).

5. Discussions

By separating the contribution due to epi-thermal neutrons through the use of Gd shielding, we succeeded in deriving a thermal-neutron capture cross-section of 1.11 ± 0.04 barns with an uncertainty of 3.6%. As a result, the resonance integral was found to be 10.5 ± 0.6 barns when the cut-off energy E_c was 0.133 eV. This resonance integral was re-evaluated at

Table 9. Present result of the half-life of ^{94}Nb together with the previously reported data.

Author	Half-life $\times 10^4$ (yr)	Method	Ref.
Present Work	**2.00 ± 0.15**	Activation & Mass analysis	
He (2012)	2.04 ± 0.04	Activation & Mass analysis	[4]
Schuman (1959)	2.03 ± 0.16	Activation & Mass analysis	[34]
Rollier (1955)	1.77 ± 0.44	Activation	[35]
Douglas (1953)	2.2 ± 0.5	Activation	[36]
Hein (1952)	>5	Activation	[37]

a cut-off energy of 0.5 eV as defined for comparison with other reported values. Considering 0.45 gσ_0 for I_0' with Eq. (4), the resonance integral I_0 above 0.5 eV was calculated as 10.1 ± 0.6 barns. The present result provides convergence for the previously reported data, which have large uncertainties and discrepancies. Among the reported data, Krane separately derived the cross sections for the generation of isomer ^{94m}Nb and ground state ^{94g}Nb by the activation method using the TRIGA reactor at the Oregon State University [14]. In the process of deriving the cross sections for these states separately, Krane obtained the thermal-neutron capture cross-section for ^{94g}Nb to be 1.06 ± 0.04 barns including the contribution of ^{94g}Nb production through the isomer ^{94m}Nb. Krane's method was almost the same as the present one. The present result agreed especially well with the value reported by Krane within the limits of uncertainties, and also with the recent compilations [2,3]. Furthermore, the resonance integral 10.5 ± 0.6 barn in the present work agreed well with 10.8 ± 1.1 barn by Krane within the limits of uncertainties.

The sensitivity parameter s_0 for epi-thermal neutrons was found to be 9.74 ± 0.52, which lies between that of ^{59}Co and of ^{197}Au used for flux monitors. When measuring the neutron flux components, as shown Figure 7, Nb foil or wire could be used as a neutron flux monitor to complement those monitors.

Here, a discussion is given on the half-life of ^{94g}Nb. The reported half-life data are summarized in Table 9 together with the present one. He GZ [4] *et al.* and Schuman [34] *et al.* derived the half-lives by a combination of activation and mass analyses as in the present work. The main contribution to the uncertainty is the accuracy of the isotope ratio of ^{94}Nb and ^{93}Nb. Hein [37] *et al.*, Douglas [36] *et al.*, and Rollier [35] *et al.* made absolute measurements of specific activities of ^{94}Nb produced by activation and then derived the ^{94}Nb half-life to account for the activities. The present result agreed with the value by He GZ *et al.* [4] within the limits of uncertainties. If the present result was used for analysis, the thermal-neutron capture cross-section would be changed by 2% at most. When deriving the resonance integral, the reaction–rate ratio R/R' is taken, thus the change in the half-life cancels and the result of the resonance integral remains unchanged. To reduce the uncertainty of the isotope ratio ^{94}Nb/^{93}Nb, we had considered either (1) longer neutron irradiation or (2) improvement of detection accuracy in the mass spectrometry. However, for the following reasons it is difficult to apply the items to the actual measurement. Regarding the first point, it would be better to obtain a larger amount of ^{94}Nb by increasing the neutron irradiation period to be much longer than at present, but on the other hand, at the same time a large amount of ^{182}Ta is also produced. As seen in *Sec.* 3.3, ^{182}Ta has a relatively long half-life (114.43 days [22]) and emits numerous gamma rays. It would subsequently take a much longer cooling-time than 2 years in order to accurately measure the radioactivity of ^{94}Nb. Concerning the second points, it is conceivable to improve the precision of mass spectrometry of Nb by an order of magnitude to 10^{-7}. For this purpose, it is necessary to examine adding new additives such as silica gel to the Nb sample, but this would take additional efforts. Here, we leave it as work for future mass analyses.

6. Conclusion

The thermal-neutron capture cross section σ_0 and resonance integral I_0 for the nuclide ^{93}Nb important for decommissioning were measured by an activation method and the half-life of ^{94}Nb by mass analysis. Niobium-93 samples were irradiated with the use of the hydraulic conveyer installed in the research reactor in Institute for Integral Radiation and Nuclear Science, Kyoto University. Gold-aluminum and cobalt-aluminum alloy wires were used to measure thermal-neutron fluxes and epi-thermal *Westcott*'s indexes at the irradiation position. A 25-μm-thick gadolinium foil was used to differentiate reactions ascribed to thermal- and epi-thermal neutrons. Its thickness provided a cut-off energy of 0.133 eV. Gamma-ray spectroscopy was applied to measure the induced radioactivity of monitors and ^{94g}Nb. By analysis based on *Westcott*'s convention, the σ_0 and I_0 values were determined as 1.11 ± 0.04 barns and 10.5 ± 0.6 barns, respectively. Following the γ-ray measurements, mass analysis was applied to the Nb samples to obtain the reaction rate. By combining the reaction rates obtained by both γ-ray spectroscopy and mass analysis, the half-life of ^{94}Nb was also determined as (2.00 ± 0.15) $\times 10^4$ years, which is in agreement with the recently reported value within the limit of uncertainty.

Acknowledgments

This work has been carried out in part under the Visiting Researcher's Program of the Institute for Integrated Radiation and Nuclear Science, Kyoto University. The authors would like to express their appreciation to the staff of Kyoto University for their support: Prof. Jun-ichi HORI, Dr. Yuichi OKI, Messrs Daisuke MAKI, Ryo OKUMURA, Yuto IINUMA and Hisao YOSHINAGA. One of the authors (S. Nakamura) would like to express my gratitude to Dr. Osamu IWAMOTO and Dr. Hideo HARADA of JAEA for their constructive comments, suggestions and encouragement, and also thank Dr. James SMALLCOMBE of JAEA for proofreading the revised manuscript.

ORCID

Shunsuke Endo http://orcid.org/0000-0001-9100-6763
Atsushi Kimura http://orcid.org/0000-0002-1942-1724

References

[1] Application of the concepts of exclusion, exemption and clearance. No. RS-G-1.7. Austria: International Atomic Energy Agency; 2004, Report no. RS-G-1.7.
[2] Mughabghab SF. Atlas of neutron resonances. 6th ed. Netherlands: Elsevier Science; 2018.
[3] Shibata K, Iwamoto O, Nakagawa T, et al. JENDL-4.0: a new library for nuclear science and engineering. J Nucl Sci Technol. 2011;48(1):1–30. DOI:10.1080/18811248.2011.9711675
[4] He GZ, Jiang S, Zhou ZY, et al. Precise half-life measurement for the ground state of ^{94}Nb. Phys Rev C. 2012;86:014605.
[5] Abriola D, Sonzogni AA. Nuclear data sheet for A=94. Nucl Data Sheets. 2006;107(9):2423.
[6] Anderson H, Fermi E, Wattenberg A, et al. Method for measuring neutron-absorption cross sections by the effect on the reactivity of a chain-reactive pile. Phys. Rev. 1947;72(1):16–23. DOI:10.1103/PhysRev.72.16
[7] Seren L, Friedlander HN, Turkel SH. Thermal Neutron Activation Cross Section. Phys. Rev. 1947;72(10):888–901.
[8] Harris SP, Muehlhause CO, Rasmussen S, et al. Pile neutron absorption cross sections. Phys. Rev. 1950;80 (3):342–344. DOI:10.1103/PhysRev.80.342
[9] Colmer FCW, Littler DJ. Pile neutron absorption cross sections of some of the elements. Proc. Physical Society (London), Section A. 1950;63 (10):1175.
[10] Tattersall RB, Rose H, Pattenden SK et al. Pile Oscillator Measurements of Resonance Absorption Integrals. J Nucl Energy A: React Sci. 1960;12(1–2):32–46.
[11] Druschel RE, Halperin J. The thermal neutron capture cross sections and resonance integrals of ^{93}Nb and ^{94}Nb. 1968; vOL. 2 ORNL-(4306). Oak Ridge National Laboratory Progressreport (U.S.A).
[12] Schuman R. Activation cross sections of Nb-93 and Nb-94. 1969 . Washington AEC Office Reports (U.S. A.):No.1136, p.5.
[13] Serpa MR. Total neutron cross section on ^{94}Nb Master's thesis. (Idaho State University).
[14] Krane KS. Neutron capture cross sections of Nb 93. Phys Rev. C, Nucl Phys. 2019;100(3):034613.
[15] Westcott CH, Walker WH, Alexander TK. Proceedings of Second International Conference Peaceful Uses Atomic Energy; 1958 Sep 1-13; Geneva, Switzerland; United Nations Publication; 1958. 202, 16: 70–76.
[16] Walker WH, Westcott CH, Alexander TK. Measurement of Radiative Capture Resonance Integrals in a Thermal Reactor Spectrum, and the Thermal Cross Section of Pu-240. Can J Phys. 1960;38(1):57–77.
[17] Nakamura S, Shibahara Y, Shunsuke E, et al. Thermal-neutron capture cross sections and resonance integrals of the ^{243}Am(n,γ)^{244g}am and ^{243}Am(n,γ)$^{244m+g}$Am reactions. J Nucl Sci Technol. 2021;58(3):259–277.
[18] Sekine T, Baba H. Self-shielding and burn-out effects in the irradiation of strongly-neutron -absorbing material. J Radioanalytical Chem. 1978;45(1):155–167.
[19] Scherbakov O, Harada H. Resonance self-shielding corrections for activation cross section measurements. J Nucl Sci Technol. 2002;39(5):548–553.
[20] Nakamura S, Shibahara Y, Kimura A, et al. Measurements of thermal-neutron capture cross-section of cesium-135 by applying mass spectrometry. J Nucl Sci Technol. 2020;57 (4):388–400. DOI:10.1080/00223131.2019.1691077
[21] Institute for Integrated Radiation and Nuclear Science, Kyoto University [Internet]. Osaka: Kyoto University; [cited December 14th , 2021]. Available from: https://www.rri.kyoto-u.ac.jp/en/facilities/kur
[22] Firestone RB, Shirley VS, Baglin CM, et al. Table of Isotopes. 8th. New York: John Wiley and Sons; 1995.
[23] Hayodom V, Boonkong W, Mahapanyawong S, et al. Resonance integral measurements. Atomic Energy for Peace, Bangkok Reports Thailand. 1969; Thai-AEC-23.
[24] Lesage L, Sher R. Measurement of Infinite Dilution Capture Resonance Integrals with a Moxon-Rae Detector. In: Chernick, J. Proceedings of the national topical meeting on reactor physics in the resonance and thermal regions; San Diego (USA); 1966. Vol. 2: p. 175.
[25] Feiner F Resonance integrals of manganese, hafnium, and niobium. USA: Knolls Atomic Power Lab.; 1961, report series no.2000-16, vol. (I.3).
[26] Macklin RL, Pomerance HS, Arfken G, et al. Resonance Capture Integrals. The first international conference on peaceful uses atomic energy; 1955 Aug 1-20; Geneva, Switzerland; 5: 96.
[27] Platzner IT. Modern isotope ratio mass spectrometry. Chichester: Willey; 1997.
[28] Shibahara Y, Kubota T, Fujii T, et al. Analysis of cesium isotope compositions in environmental samples by thermal ionization mass spectrometry-1. A preliminary study for source analysis of radioactive contamination in Fukushima prefecture. J Nucl Sci Technol. 2014;51 (5):575–579. DOI:10.1080/00223131.2014.891954
[29] Shibahara Y, Kubota T, Fujii T et al. Determination of isotopic ratios of plutonium and uranium in soil samples by thermal ionization mass spectrometry. J Radioanal Nucl Chem. 2016;307(3):2281–2287.
[30] Shibahara Y, Kubota T, Fujii T, et al. Analysis of cesium isotope compositions in environmental samples by thermal ionization mass spectrometry-3. Measurement of isotopic ratios of Cs in soil samples obtained in Fukushima prefecture. J Nucl Sci Technol. 2017;54 (2):158–166. DOI:10.1080/00223131.2016.1223560

[31] Shibahara Y, Hori J, Takamiya K et al. High precision analysis of isotopic composition for samples used for nuclear cross-section measurements. ND2016: international Conference on Nuclear Data for Science and Technology; 2016 Sep 11-16; Brugge (Belgium). EPJ Web of Conferences; 2017. vol. 146. P. 03028.

[32] Shibahara Y, Nakamura S, Uehara A, et al. Measurement of cesium isotopic ratio by thermal ionization mass spectrometry for neutron capture cross section studies on ^{135}Cs. J Radioanal Nucl Chem. 2020;325:155–165.

[33] Kramida A, Ralchenko Y, Reader J et al.2021NIST Atomic Spectra Database (ver5.9)[Online]. Availablehttps://physics.nist.gov/asd

[34] Schuman RP, Goris P. Half-life and decay of niobium-94. J Inorg Nucl Chem. 1959;12(1–2):1–5.

[35] Rollier MA, Seland E, Morpurgo A, et al. Half-life and radiations of the long-lived isotope of niobium (^{94}Nb). Acta Chem Scand. 1955;9(1):57–67.

[36] Douglas DL, Mewherter AC, Schuman RP. A long-lived activity in neutron-irradiated niobium. PR. 1953;92(2):369–371.

[37] Hein RE, Fowler CM, McFarland RH. Search for long-lived Nb^{94}. PR. 1952;85(1):138–139.